Comparison of soil water content estimation equations using ground penetrating radar

Published Version:
Comparison of soil water content estimation equations using ground penetrating radar / Anbazhagan P.; Bittelli M.; Pallepati R.R.; Mahajan P.. - In: JOURNAL OF HYDROLOGY. - ISSN 0022-1694. - STAMPA. - 588:(2020), pp. 125039.1-125039.9. [10.1016/j.jhydrol.2020.125039]

Availability:
This version is available at: https://hdl.handle.net/11585/765737 since: 2020-07-11

Published:
DOI: http://doi.org/10.1016/j.jhydrol.2020.125039

P. Anbazhagan, Marco Bittelli, Rao Raghuveer Pallepati, Puskar Mahajan

Comparison of soil water content estimation equations using ground penetrating radar

Journal of Hydrology Volume 588, September 2020, 125039

Abstract

Soil water content (SWC) has an important impact on many fundamental biophysical processes. The quantification of SWC is necessary for different applications, ranging from large−scale calibration of global-scale climate models to field and catchemnt scale monitoring in hydrology and agriculture. Many techniques are available today for measuring SWC, ranging from point scale soil water content sensors to global scale, active and passive, microwave satellites. Geophysical methods are important methods used for several decades to measure SWC at different scales. Among these methods, Ground Penetrating Radar has been shown to be one of the most reliable and promising ones. Soil water content measurement using Ground Penetrating Radar requires the applications of parametric equations that will convert the measured dielectric permittivity to water content. While several studies have been performed to test equations for soil water content sensors such as Time Domain Reflectometry, a few studies have been performed to test different formulae for application to Ground Penetrating Radar. In this study, we compare available formulae for converting dielectric permittivity obtained from detailed laboratory scale measurement of reflected waves using Ground Penetrating Radar. Four soils covering a wide range of textures were used and the measured soil water contents were compared with values obtained from gravimetric measurements. Results showed that the dielectric mixing model of Roth (1990) provided the best fit both for individual soil textural classes, except for sandy soils. However, for all data combined the dielectric mixing model performed much better with significant difference in coefficient and determination and Root Mean Square Error (RMSE = 0.028 m^3 m^{-3} and R^2= 0.888). Empirical equations developed from calibration of TDR performed poorly when applied to estimation of soil water content obtained from GPR. Differences in sample volume, frequency of operation and data analysis between GPR and TDR, suggest to use more flexible and robust electromagnetic mixing formulae, allowing for incorporating the dielectric properties of constituents materials and geometrical features of the media. Sensitivity analysis was then performed to provide detailed information for the most accurate application of the selected dielectric model.

Keywords: Ground Penetrating Radar, Soil Water Content, Dielectric Mixing Models, Empirical Equations, Sensitivity Analysis

*Highlights (3 to 5 bullet points (maximum 85 characters including spaces per bullet point)

Highlights

- Accurate measurement of dielectric permittivity with reflected waves GPR was obtained
- Evaluation of Water Content Estimation Equations using wide range of textures
- Identification of best fit equation and critical analysis of current equations
- Sensitity Analysis of the best fit model

Comparison of Soil Water Content Estimation Equations using Ground Penetrating Radar

Anbazhagan P.[1], Marco Bittelli[2,*], Rao Raghuveer Pallepati[1] and Puskar Mahajan[1]

[1]Department of Civil Engineering, Indian Institute of Science, Bangaluru, India

[2]Department of Agricultural and Food Sciences, University of Bologna, Italy

* Corresponding author. Department of Agricultural and Food Sciences, University of Bologna, Italy, Viale Fanin, 44, 40100 Bologna, Italy. Phone:+39-051-2096644, Fax:+39-051-2096641,E-mail: marco.bittelli@unibo.it; (M. Bittelli)

1. Introduction

Soil water content (SWC) is a fundamental property affecting a large variety of processes relevant to hydrology, agricultural sciences, engineering and soil sciences. Over the last decades many techniques have been developed to measure SWC at different temporal and spatial scales. Bittelli (2011) provided a review describing the most common methods available for measuring SWC. Among geophysical techniques, Ground Penetrating Radar (GPR) is a powerful and promising one. GPR has the advantage of covering larger areas with respect to point−based measurements typical of soil moisture sensors such as Time Domain Reflectometry (TDR), filling the gap between point scale and large scale satellite−based measurement. Soil water content can be obtained by performing different types of analysis and methods using GPR. Huisman et al. (2003) and Klotzsche et al. (2018) presented reviews about advances in applications of GPR, for measurement of SWC. In their reviews they discuss available methodologies, including continuous multi−offset measurements, off−ground measurements, three−dimensional measurements, vertical radar profiling, modelling and inverse methods.

When the value of dielectric permittivity for the material under test is obtained from GPR, relationships must be employed to convert permittivity to volumetric SWC. Commonly, the relationships used for GPR are the ones derived from the calibration of TDR. Since both TDR and GPR are volumetric measurements, during the calibration measurement of bulk density is necessary to convert the mass−based gravimetric measurement to volume−based soil water content. Many equations were derived over the years.

One of the most widely used is the one by Topp et al. (1980), which is a third order polynomial. The authors used TDR to measure the dielectric permittivity for a range of granular samples placed in a coaxial transmission line and they estimated an error of 0.013 m^3 m^{-3}. Ledieu et al. (1986) proposed an equation where the calibration of TDR was performed against gamma−ray attenuation, an accurate technique used for measuring water content. The calibration equation accounted for the change in bulk density of the specimen. Later, Roth et al. (1992) proposed calibration functions for mineral, organic and magnetic soils. Malicki et al. (1996) also presented a formulation accounting for bulk density. These are empirical equations.

Roth et al. (1990) proposed a dielectric mixing model based on theoretical considerations. This model includes: 1) the effect of bulk density (by accounting for soil porosity), 2) a geometrical parameter describing the orientation of soil particles with respect to the electric field and 3) the values of dielectric permittivity for the solid, liquid and gas phase. While the gas phase permittivity is constant, the solid phase permittivity changes with soil minerals, while the liquid phase permittivity is temperature dependent (assuming constant or narrow-band frequency).

The dielectric mixing model of Roth et al. (1990) belongs to the family of the electromagnetic mixing models, which are applied to a large variety of media including snow, ice, emulsions and biological materials. One of the most exhaustive description and review about the theory of electromagnetic mixing formula was presented by Sihvola (1999). As pointed out by Sihvola (1999), heterogeneous mixtures (such as a soil) have properties that depend upon its constituents but differ from the original components. Although the dielectric properties of a mixture are an average of the components permittivities, often the whole character of the dielectric is changed by the mixing process. An important aspect of the effect of the mixing process is the geometrical orientation of the inclusions (particles) with respect to the electric field and their depolarisation factors, which depend on the shape of the inclusions.

The relationships currently used for GPR applications were derived from experiments performed with TDR and applied to various studies. Weihermuller et al. (2007) used the Topp et al. (1980) formula to derive water content from GPR. Gerhards et al. (2008) and Steelman et al. (2012) derived SWC from multiple transmitter and receiver GPR, employing the Roth et al. (1990) dielectric mixing model. However, there are many differences between TDR and GPR, in terms of frequency of operation, sampling volume, data analysis and interpretation. Therefore there is the need to test the current equations applied to GPR. Only a few studies have been performed.

Lambot et al. (2004) estimated SWC directly from GPR, using a soil−specific empirical model (third order polynomial) similar to Topp's equation. However, their experiment was limited to a sand box with only a sandy sample as testing material. Steelman and Endres (2011) presented a comparison among petrophysical relationships for application to GPR. They concluded that the general empirical equation by Roth et al. (1992) provided the best fit for the sandy loam soil. When the entire data set was analyzed, they found that the Topp et al. (1980) and Roth et al. (1992) relationships provided the most accurate estimates. When the dielectric mixing and effective media models were tested, the Roth et al. (1990) equation provided the best fit, but with small improvement with respect to the empirical equations.

However, Steelman and Endres (2011) used permittivity data, to test the equations, obtained from GPR using the Common Midpoint (CMP) sounding method. With this method, stacking velocity fields are extracted from multi−offset radar soundings at a fixed central location. Yet, CMP−derived velocity estimates are generally characterized by low resolution and high uncertainty (Tillard and Dubois, 1995; Lambot et al., 2004). The success of the measurements depends on the presence of clearly reflecting layers in the soil. For this reason the calibration equations derived from dielectric permittivity obtained from CMP may be affected by low resolution and high uncertainty.

The travel time of the reflected GPR wave depends on the depth of the reflector and the mean dielectric permittivity above the reflector. In general, in field applications the reflectors depth are unknown, requiring the use of techniques to derive the dielectric permittivity, described in the review by Klotzsche et al. (2018). However, for controlled studies on calibration equations, it is more accurate to perform GPR measurements with a strong reflector installed at a known depth to derive an accurate travel time, as performed by Lambot et al. (2004). The authors performed detailed radar measurements carried out in controlled laboratory conditions on a tank filled with a disturbed sandy soil. The purpose of their paper was to test forward GPR modelling, therefore to test the modelling analysis they selected an accurate and robust approach to obtain travel time in controlled laboratory conditions.

In this study, the performance of various published physical relationships used to obtain soil water content estimates from GPR, were evaluated. Dielectric permittivities of the materials under test were obtained by using a tank filled with disturbed soil samples and with a metal reflector installed at a known depth. Four different materials were tested ranging from sand to kaolinite clay, to obtain a broad range of textures. Variations in water content and densitis were independently measure for comparison. Sensitivity analasis of the best fit model was then performed.

2. Theory

Ground Penetrating Radar reflections occur when there are significant changes in dielectric permittivity. In natural conditions they can ben sedimentation layers, groundwater tables, rocks stratification. In man−made structures they can be archaelogical remains, pipes used for utilities, cavities, roads layering. Since SWC strongly affects the dielectric permittivity of porous media, GPR is an effective technique to measure SWC. One of the most common techniques for measuring SWC is based on derivation of dielectric permittivity from travel time analysis.

The velocity v (m s^{-1}) of an electromagnetic wave, is affected by the dielectric permittivity ϵ, and the magnetic permeability μ, as:

$$v = \frac{c}{\sqrt{\mu\epsilon}} \tag{1}$$

where c is the speed of light, 2.997×10^8 (m s^{-1}). From a mechanical standpoint, the velocity v of an electromagnetic wave traveling through a space of length d (m), is given by:

$$v = \frac{2d}{t} \tag{2}$$

where t is time (s). For a reflected wave, the number 2 in front of the length is included because the wave is reflected back to the receiving antenna. For most soils μ_r is equal to 1 (Roth et al., 1992), therefore Eqn. 1 can be written as:

$$v = \frac{c}{\sqrt{\epsilon}} \tag{3}$$

By equating the definitions of velocity:

$$\frac{c}{\sqrt{\epsilon}} = \frac{2d}{t} \tag{4}$$

and solving for ϵ:

$$\epsilon = \left(\frac{ct}{2d}\right)^2 \tag{5}$$

Equation 5 allows for obtaining the dielectric permittivity by measuring the travel time t, since the position of the reflecting plane d and the speed of light c are known. When the material is a composite mixture such a soil, we refer it as bulk dielectric permittivity (ϵ_b). Knowledge of the distance between the antenna and the reflector d, allows for obtaining the travel time and the dielectric permittivity, this method is usually called the $two-way$ travel times analysis (Pereira et al., 2005).

2.1. Soil Water Content relationships

2.1.1. Empirical Equations

The empirical relationship by Topp et al. (1980) is:

$$\theta = -5.3 \times 10^{-2} + 2.92 \times 10^{-2}\epsilon_b - 5.55 \times 10^{-4}\epsilon_b^2 + 4.3 \times 10^{-6}\epsilon_b^3 \tag{6}$$

where θ is the volumetric water content (m^3 m^{-3}) and ϵ_b is soil bulk dielectric permittivity. The authors fitted the third order polynomial to TDR data collected in a coaxial transmission line for four soils.

Ledieu et al. (1986) developed an equation obtained from calibrating TDR against SWC data obtained from gamma−ray attenuation. Since dielectric permittivity is density dependent they also included the bulk density. They stated that their procedure and calibration equation had accuracy of less than 1 %. However the experiment was performed only on one sample of sand. The equation proposed is:

$$\theta = 0.1138\sqrt{\epsilon_b} - 0.1758 \tag{7}$$

Roth et al. (1992) proposed three different empirical equations for mineral, organic and magnetic soils. The equation for mineral soil is also a third-order polynomial similar to Topp's equation, but with different coefficients and a prediction error of 0.015 m^3 m^{-3}:

$$\theta = -7.28 \times 10^{-2} + 4.48 \times 10^{-2}\epsilon_b - 19.5 \times 10^{-4}\epsilon_b^2 + 36.1 \times 10^{-6}\epsilon_b^3 \tag{8}$$

2.1.2. Electromagnetic Mixing Formulas

Electromagnetic mixing formulae relate the value of the individual permittivities of the mixture components to their volumetric fractions. A widely used class of mixing models are called power−law models (see Sihvola (1999), page 166), where a certain power of the permittivity is averaged over volume weights:

$$\epsilon_b^\beta = f\epsilon_i^\beta + (1-f)\epsilon_j^\beta \tag{9}$$

where ϵ_i and ϵ_j are the generic dielectric permittivities of a two phase systems. In the Birchak et al. (1974) equation, the parameter β is equal to 1/2. Another known model is the Looyenga (1965) formula, where β is equal to 1/3. Later, Roth et al. (1990), extended the power−law model to compute the bulk dielectric permittivity as a weighted sum of the dielectric permittivity of each soil phase:

$$\epsilon_b = (\phi_s \epsilon_s^\alpha + \theta \epsilon_l^\alpha + \phi_g \epsilon_g^\alpha)^{1/\alpha} \tag{10}$$

where ϕ_s, θ and ϕ_g are the solid, liquid and gas phase volumetric fractions. The corresponding dielectric permittivities are ϵ_s, ϵ_l and ϵ_g, while α is the parameter describing the geometry of the medium with relation to the applied electric field. The volumetric solid fraction can be also written as $\phi_s = (1 - \phi_f)$, where ϕ_f is the porosity and the volumetric fraction of the gas phase as $\phi_g = (\phi_f - \theta)$. Using these relationships and substituting into Eqn.10, leads to:

$$\theta = \frac{\epsilon_b^\alpha - \left[(1 - \phi_f)\epsilon_s^\alpha + \phi_f \epsilon_g^\alpha\right]}{\epsilon_l^\alpha - \epsilon_g^\alpha} \tag{11}$$

The liquid phase dielectric permittivity is temperature dependent with:

$$\epsilon_l = 78.54 \times (1 - (4.579 \times 10^{-3} \times \Delta T)) \tag{12}$$

where T is temperature in Celsius and $\Delta T = T - 25$. To use this equations, knowledge of porosity (which can be obtained from measurement of bulk density) and dielectric permittivity of the solid phase is needed. Porosity is obtained from measured bulk density by:

$$\phi_f = 1 - \frac{\rho_b}{\rho_s} \tag{13}$$

where the density of the solid phase (ρ_s) was assumed to be equal to 2.65 g cm^{-3}.

The sum of the different volume−weighted permittivities can be extended to include the contribution of organic matter in organic soils, or ice in partially frozen soils (Bittelli et al., 2004). Table 1 provides dielectric permittivity values for different materials (Daniels, 2004). In this study we used the following values: $\epsilon_s = 4$, ϵ_l was computed with Eqn. 12 at 25 °C, $\epsilon_g = 1.005$ and $\alpha = 0.5$.

Table 1: Dielectric permittivity of materials at 100 MHz. From Daniels (2004)

Material	Dielectric permittivity
Vacuum	1
Air	1.0005
Fresh water	$78.54 \times (1 - 4.579 \times 10^{-3}(T - 25))$
Fresh water ice	3.2
Quartz	4−6
Concrete dry	4−10
Sand Dry	2−6
Sandstone dry	2−5
Soil Dry Clay	4−10
Granite Dry	5
Limestone dry	7

The selection of these four models was also based on previous results obtained by Steelman and Endres (2011) as discussed above.

The disadvantages of using empirical models are manyfolds: a) the models are not derived from theoretical considerations regarding the interactions between the electric field and the media therefore they are theoretically less robust, b) the parameters are obtained from fitting the equations over a given data set, therefore if the model is applied to other materials they may fail and c) the coefficients of empirical models are commonly fixed values. The opposite is true for dielectric mixing models where: a) the model are based on theoretical considerations where the parameters represent measureable physical properties, b) the parameters can be selected based on measured properties of the media (for instance the mineralogical composition of the solid phase) or from existing tables, and c) the parameters can be used as fitting parameters for a specific study, allowing for flexibility in the equation form.

3. Material and Methods

Four different soils were used in this study, namely sand, sandy loam, loamy sand and kaolinite clay. Samples were collected from the Tumkur district, Karnataka, India. The soil samples were collected from the top 25 cm of soil. The experiments were conducted at laboratory temperature of 25 °C. This value was used for correcting the dielectric permittivity of the liquid phase in the dielectric mixing models (Eqn.12), which provided a value of $\epsilon_l =$ 78.54. The tested soils were cleaned for presence of organic material like grass, leaves etc. and sieved with a 2.5 mm size sieve. Figure 1 shows a schematic of the experimental setup, while Figure 2 shows two photographs of the experimental setup.

FIGURE 1

FIGURE 2

The soil was placed into a plastic tank (with base 0.6 m $\times$ 0.4 and 0.3 m height) for a total volume of 0.072 m^3, with a reflecting metal plate at the bottom. The distance for travel time calculation between the antennas and the reflecting metal plate was $d \simeq 0.3$ m. According to the manufacturer (Mala Inc.) the antennas are positioned at the bottom of the GPR, where a plastic lower case of a few mm thickness separate the antennas from the soil. Therefore a value of $d \simeq 0.3$ is the correct physical distance between the antennas and the metal reflector.

The distance between the transmitting and receiving antennas is 0.1 m. Materials underneath the metal sheet have no influence on the measured backscattered signal (Lambot et al., 2004).

The soil was prepared by following the ASTM D1557 12 standard for laboratory compaction (ASTM, 2015). A fixed amount of water was added to a specific mass of soil, and mixed to obtain uniform distribution of water. Specifically: a) the sand was packed into the tank volume of 0.072 m^3, at an average dry bulk density of 1593 kg m^{-3}, corresponding to a dry mass of 114.7 kg; b) the sandy loam at an average bulk density of 1561 kg m^{-3}, corresponding to a dry mass of 112.4 kg; c) the loamy sand at an average bulk density of 1571 kg m^{-3}, corresponding to a dry mass of 113.1 kg and d) the kaolinite clay was packed at an average bulk density of 1175 kg m^{-3}, corresponding to a dry mass of 84.6 kg.

The soil samples were then placed into the tank and packed to the densities described above, in three incremental layers of 0.1 meters each, of equal mass. The layers in the figure do not represent different soil types, but the layers used for packing. The packing was done by layering to achive a uniform density. GPR antenna was then placed on the top of the plastic box and readings were taken in time-triggering mode.

Subsequently, the soil was removed from the tank and fixed amounts of water were added to increase water content. The same packing procedure was then repeated, therefore everytime the soil was prepared and repacked into the tank, for each SWC measurement. The mixing of soil and water was done by hand, with scoops and shavels, into a separate larger open container. The soil was then enclosed into the container to avoid evaporation and let equilibrate for 24 hrs, to allow for water redistribution and equilibration within the sample. Mixing was then performed again. To test the effectiveness of the mixing, periodically gravimetric tests of the mixtures during the mixing and equilibration processes were also performed (ASTM, 2015).

This procedure was followed, not only because it is a standard ASTM, but also beacuse it was not possible to increment water content within the tank by either percolation or capillary rise. At the bottom of the tank a reflecting metal plate was positioned for GPR analysis, therefore we could not control the lower boundary condition for percolation or capillary rise with installation of either ceramic or porous plates. Moreover, percolation of water into a tank often results in preferential flows of water along the walls and preferential pathways, resulting in non−homogeneous distributions. For these reasons, the soil was repacked each time for each individual SWC measurement. Sometime, after adding water to the target amounts, the densities underwent some variations during packing.

However, to verify water content and bulk density values and to test SWC equations, after the GPR measurement was performed, three soil samples were collected in metal rings from the center of the tank (below the positions of the GPR antennas) and independent gravimetric SWC and bulk densities were measured. Although special care was payed to pack the soil at the same density, since the volume of the tank and the soil mass were relatively large, it was not possible to repack the soil exactly at the same densities, therefore variations in bulk densities were recorded during the measurement. These variations were included for each measurements into the SWC models that allowed to include porosity, namely the empirical model of Ledieu et al. (1986) and the dielectric mixing model of Roth et al. (1990).

3.1. Ground Penetrating Radar measurements

The GPR was a Mala Inc., with a 800 MHz shielded antennas. The setup was the following: time window = 38.8 ns, depth = 0.3 m, sampling frequency = 8230.951172 MHz and antenna separation = 0.1 m. The data were analysed using the software Prism 2 (Radar System Inc.) and Reflex (Sandmeier, 2019). The acquisition was performed in time−based trace triggering mode.

Figure 3 shows an example of radargrams showing the reflector depth. The reflection in the upper part of the signal are the typical air and ground wave. The transmitting antenna propagates waves giving rise to an air wave that travel directly from the transmitting to the receiving antenna. Similarly, the propagating wave give rise to the ground wave. The upper part of the radargram shows the air and ground wave. Figure 3 shows the strong reflection of the metal reflector. The graph does not display any unit on the x−axis since the measurement is performed in time−triggering mode. Detailed analysis on single trace analysis (A−scan) is explained below.

FIGURE 3

Depth penetration is controlled by the dielectric permittivity and electrical conductivity of the sample. In fine textured soils, in particular in clay soils, the signal can be highly attenuated. Moreover, in fine textured samples relaxation processes (such as Maxwell−Wagner or double layer polarization) may determine additional dissipation processes and further attenuation of the signal (Schwing et al., 2013).

The procedure to identify the reflections was based on the calibration procedure presented by Pereira et al. (2005). The authors pointed out that one of the main problems related to GPR technology is that the technical information provided by the different companies is practically inexistent. The lack of information for the different parameters for antenna emissions and emitted signal is a serious difficulty for data interpretation. For instance, the authors showed that the rate of drift of the signal was not exactly the same for the three antennas under test, operating at 500, 800 and 1000 MHz. Indeed, the time base of GPR measurements is also not exactly determined and it may shows a significant drift due to a temperature difference between the instrument electronics and the ambient temperature. Accordingly, as suggested by the authors we increased the warming time of the GPR to 30 minutes to equilibrate with the laboratory temperature. Since the authors used the same GPR manufacturer used in this study (Mala Inc.), we employ their procedure to identify the time zero parameter.

An exact definition of time zero in field conditions is very difficult if not impossible, since it is not a constant value but depends on the investigated material and the antenna set up configuration (Sandmeier, 2019). However, when the physical distance of the reflector and the distance between the antenna are known, it is possible to determine the time zero for the investigated material. An automatic and stable static correction (definition of time zero) may be done either on the first negative, first zero crossing or first positive peak (Sandmeier, 2019). Pereira et al. (2005) suggested to use the first positive peak (Fig. 4 in (Pereira et al., 2005)) for the 800 MHz antenna.

Figure 4 shows an example of a trace and identification of the reflection for computation of travel time. The lower plate shows the complete trace acquired during the experiment and the upper plate a zoom over the relevant section. The origin was fixed by starting off at the greatest amplitude value from the first positive semiperiod peak. After obtaining the travel time, the bulk dielectric permittivity was then computed as detailed above.

FIGURE 4.

3.2. Error Analysis

The accuracy of the volumetric soil water content estimates was estimated using the Root Mean Squared Error (RMSE):

$$RMSE = \sqrt{\frac{\sum_{i=N}^{N}(\theta_{meas} - \theta_{pred})^2}{N}} \tag{14}$$

where N is the total number of samples, θ_{meas} (m^3 m^{-3}) is the volumetric water content obtained from gravimetric measurements and θ_{pred} (m^3 m^{-3}) is the volumetric water content predicted by the different equations, and obtained from GPR measurement of bulk dielectric permittivity. The coefficient of determination R^2 was also used to evaluate regression equation in the scatter plot analysis.

4. Results and Discussion

The estimated volumetric water contents, θ, obtained from the different equations are presented in Figure 5 for the four different textural classes and the RMSE results are presented in Table 2. The dielectric mixing model of Roth et al. (1990) provided the best fit for the tested soils, except for the sandy loam where the Topp's and Ledieu's equations provided the best fit. However, when all the data were combined the dielectric mixing model of Roth's provided the best fit, with RMSE of 0.028 m^3 m^{-3}.

As confirmed by the values of RMSE, it is also possible to visually see the best fitting of the dielectric mixing model for the indicated textures. Considering the experimental difficulties in achieving uniform packing of wetted soil into a large tank with large amount of soils, the scatter of the experimental data is fairly small, confirming the accuracy of the experimental

Table 2: Root Mean Square Error (RMSE) (m^3 m^{-3}) for the four different soil types and all data. DMM stands for dielectric mixing model.

Relationships	sand	sandy loam	loamy sand	kaolinite clay	all data
Topp et al. (1980)	0.024	0.035	0.022	0.033	0.051
Ledieu et al., (1986)	0.023	0.035	0.025	0.030	0.052
Roth et al. (1992)	0.049	0.054	0.015	0.012	0.051
Roth et al. (1990)-DMM	0.022	0.040	0.010	0.010	0.028

procedure.

FIGURE 5

Figure 6 shows a scatter plot between the measured volumetric water contents (θ_{meas}) and the estimated corresponding values (θ_{est}). Regression equations and the coefficient of determination (R^2) are also listed in the graph for each equation. The coefficients of determination showed that the best fitting was obtained with the dielectric mixing model of Roth et al. (1990), followed by the Roth et al. (1992), the Ledieu et al. (1986) and the Topp et al. (1980), with R^2 respectively of 0.888, 0.790, 0.795 and 0.731.

With respect to the 1:1 line in the scatter plot, all models slightly overestimated lower water contents and underestimate higher water contents. It seems that SWC data obtained from GPR display a different relationship with permittivity, with respect to the TDR (Fig 6.). Somehow, this is expected since the GPR measurements explore a much larger volume of soil, with respect to the TDR probes, with larger variations in both water content and bulk density. Moreover, the GPR operates at different frequencies. The common antennas used in the field operates at lower frequency with respect to the operational frequency of the TDR.

Indeed, for all the samples combined the empirical equations obtained from TDR performed poorly, with low R^2. The better perfomance of the dielectric mixing model is due to its ability to incorporate the effect of porosity and dielectric permittivities of the individual phases. Moreover, its mathematical form allows for more flexibility in describing the data, as described in the next section (see Fig. 7 and 8).

In this study the dielectric mixing model was employed by using fixed parameters obtained from the literature. If the model was fitted to the experimental data, further improvement in SWC estimation would have been achieved.

FIGURE 6.

Indeed, note that the equations that use the value of porosity (or bulk density), such as the dielectric mixing model of Roth et al. (1990) are not always smooth lines (Fig. 5) and in particular for sand. This is due to the varying values of bulk density measured for each independent measurement of gravimetric SWC. As described above, experimentally was not possible to repack the soil at the exact same values of bulk density, therefore bulk density was measured every time the soil was repacked. The ability of estimating SWC as function of porosity is one of the reasons the dielectric mixing model performed better than the other models.Moreover, the varying bulk densities stress the experimental difficulties of preparing large amount of soil material at uniform water content and density.

Using empirical equations, such as the Topp's equation, where estimation of SWC is not density dependent, will lead to inaccurate estimation of SWC since density, in natural conditions, usually changes with depth. In agricultural conditions, where soil is subject to compaction and softening due to machines and tillage, the changes in bulk density over the growing season are significant, requiring equations that include the possibility of time and space dependent bulk density. For these reasons, there are active lines of research, where direct measurements of both SWC and bulk density are derived from TDR waveforms (Jung et al., 2013a,b; Curioni et al., 2018).

These results are consistent with the work of Gerhards et al. (2008), where they derived accurate SWC from GPR using a multiple transmitter and receiver setup, and employing the dielectrid mixing model of Roth et al. (1990). As pointed out by Sihvola (1999) the use of dielectric mixing models is preferable with respect to the use of empirical equations since they allow for incorporating dielectric properties of constituent materials and their temperature and frequency dependence. While the major dipole relaxation for water occurs at higher frequency (19 GHz), additional relaxations in soils, such as double layer or Maxwell-Wagner relaxations, may occur in the operational frequencies of GPR, depending on the selected antenna Olmi and Bittelli (2015).

Another parameter that significanly changes soil water content estimation is the parameter α, which is discussed in the next section.

4.1. Sensitivity Analysis of the dielectric mixing model

To employ the dielectric mixing model for different media it is important to quantify the effect of the individual parameters on the estimation of water content. As described above, the permittivity of the gas phase is constant, the porosity depends on bulk density, the permittivity of the liquid phase is temperature dependent (assuming a constant or narrow band frequency) and the permittivity of the solid phase depends on mineralogy.

Figure 7 depicts the variations of volumetric water content as function of permittivity for different values of α. The other parameters are kept fixed with $\epsilon_s = 2$, ϵ_l= 78,54 (at 25 °C), $\epsilon_g = 1.005$ and $\phi_f = 0.547$ (with ρ_b= 1.2 g cm^{-3}).

FIGURE 7.

The parameter α depends on the shape and orientation of the inclusions affecting the depolarisation factors, as detailed by Sivhola, (1999). Values of 1/2 was used by Birchak et al. (1974) or 1/3 by Looyenga (1965). Other values can also be selected for the power−law relationship. The domain is $-1 \leq \alpha \leq 1$, where $\alpha = 1$ for plates or other inclusions for which no depolarisation is induced, or when the electric field is parallel to the layering. $\alpha = -1$ if the field is perpendicular to the layering and $\alpha = 0.5$ for isotropic two-phase medium. Using a non−linear least square minimization algorithm, Roth et al. (1990) found an optimal value of $\alpha = 0.46$ for their experimental data, which is close to 0.5, the value obtained by Birchak et al. (1974) from theoretical reasons. While in this study the dielectric model was not calibrated and a fixed value of 0.5 was used, α can be modified if information about the soil layering is available, such as stratifications, sedimentation layers and others. Alternatively, α can also be used as fitting parameter. At decreasing values of α corresponds significantly increasing values of θ. Being the relationship non linear the variation depends on the corresponding values of permittivity.

The effect of the solid phase permittivity was also evaluated (Fig. 8). The parameters were kept fixed as for the previous analysis, with $\alpha = 0.5$, and ϵ_s was changed from 2 to 10. These values are the ones reported in Table 1, for different earth materials. Lower values are associated to dry sandstone and sand, while higher values are associated to dry clay. The increase of the solid phase dielectric permittivity determines a decrease in the estimated SWC. For this parameters set, a change from 2 to 10, determines a decrease in θ of 0.1 m^3 m^{-3}. This beahavior is due to the higher weight given to the the solid phase by an increased ϵ_s in the weighted volumetric sum, and therefore less weight to the volumetric contribution of the liquid phase. Also in this case, information regarding the mineralogical composition of the analyzed media allows for modification of this parameter.

FIGURE 8.

The effect of temperature on the liquid phase permittivity, and therefore on θ, is fairly small with estimated variations in volumetric water contents of about 0.03 m^3 m^{-3} over a temperature range between 4 and 20 °C. Finally, the effect of porosity on soil water content is about 0.06 m^3 m^{-3} over a variation of ϕ_f between 0.7 and 0.1, with increasing θ with increasing porosity. Considering that in field conditions bulk density can easily range, for instance, between 0.8 and 2.4 g cm^{-3} (corresponding to variations in porosity between 0.7 to 0.09 m^3 m^{-3}), the effect of bulk density is significant on SWC estimation.

Overall, the parameters that have a larger effect on estimated SWC with the dielectric mixing model are the exponent α, the solid phase permittivity ϵ_s and porosity ϕ_f. The first two can be used as fixed parameters with values of 0.5 and 4 respectively or used as fitting parameters. Porosity should be measured or obtained from bulk density. In absence of porosity or bulk density data, density can be obtained from TDR waveforms (Jung et al., 2013a,b; Curioni et al., 2018) or from pedotranfer functions by knowledge of textural composition (Rodriguez-Lado et al., 2015).

5. Conclusions

Different relationships to estimate SWC derived from soil permittivities obtained from a two−way GPR analysis data were compared. The GPR data were obtained in a controlled laboratory setting using a soil tank with a metal reflector positioned at a known depth, allowing for accurate determination of the soil bulk dielectric permittivity as function of varying water contents. The data were obtained for four distinct soil textural classes (sand, sandy loam, loamy sand and kaolinite clay) covering a wide range of soil moisture conditions. The physical relationships under test were empirical formulae and dielectric mixing models. Results showed that the dielectric mixing model of Roth et al. (1990) provided the most accurate estimate of volumetric soil water content for all soils, except for sandy loam. However, for all the data combined the dielectric mixing model performed much better with significant differences in the coefficient of determination and Root Meas Square Error. The performance of the dielectric mixing model could have been further improved by using the geometric parameter and the dielectric permittivity of the solid phase as fitting parameters.

Sensitivity analysis of the dielectric mixing model was performed showing that the geometric parameter α and the dielectric permittivity of the solid phase ϵ_s are the two most sensitive parameters, determining important variations in the estimation of SWC. Based on these results, these two parameters are suggested as fitting parameters to be selected if the model is fitted to data. Otherwise, the model can be successfully used without calibration, as presented in this study, by using $\alpha = 0.5$ (as also suggested by the authors) and $\epsilon_s = 4$, which is an average value for soil minerals. Overall, we suggest to employ the dielectric mixing model for estimation of SWC from dielectric permittivity obtained with GPR.

6. Acknowledgment

This study was funded by: Project Scheme for Promotion of Academic and Research Collaboration (SPARC). A Government of India Initiative. Project Title: Prediction of Soil Hydro Agricultural Properties using Ground Penetrating Radar for Improving Agricultural Practice (Proposal ID: 375). Responsible: Prof. Anbazhagan P., Department of Civil Engineering, Indian Institute of Science, Bangaluru, India.

References

ASTM, 2015. Standard test methods for laboratory compaction characteristics of soil using modified effort. ASTM D1557 12 , West Conshohocken, PA.

Birchak, J.R., Gardner, L.G., Hipp, J.W., Victor, J., 1974. High dielectric constant microwave probes for sensing soil moisture. Proceedings of the IEEE 62, 93–98.

Bittelli, M., 2011. Measuring soil water content: A review. Hort. Tech. 48, 1–15.

Bittelli, M., Flury, M., Roth, K., 2004. Use of dielectric spectroscopy to estimate ice content in frozen porous media. Water Resour. Res. 40, doi:10.1029/2003WR002343.

Curioni, G., Chapman, D.N., Pring, L.J., Royal, A.C.D., Metje, N., 2018. Extending tdr capability for measuring soil density and water content for field condition monitoring. Geotech. J. 144, 1–15.

Daniels, D.J., 2004. Ground Penetrating Radar. Institution of Electrical Engineers (IEE), Radar, Sonar and Navigation Series, London.

Gerhards, H., Wollschlager, U., Yu, Q., Schiwek, P., Pan, X., Roth, K., 2008. Continuous and simultaneous measurement of reflector depth and average soil-water content with multichannel ground-penetrating radar. Geophysics 73, J15–J23.

Huisman, J.A., Hubbard, S.S., Redman, J.D., Annan, A.P., 2003. Measuring soil water content with ground penetrating radar: A review. Vadose Zone J. 2, 476–491.

Jung, S., Drnevich, V.P., Najm, M.R.A., 2013a. New methodology for density and water content by time domain reflectometry. Geotech. J. 139, 659–670.

Jung, S., Drnevich, V.P., Najm, M.R.A., 2013b. Temperature corrections for time domain reflectometry parameters. Geotech. J. 139, 671–683.

Klotzsche, A., Jonard, F., Looms, M.C., van der Kruk, J., Huisman, J.A., 2018. Measuring soil water content with ground penetrating radar: A decade of progress. Vadose Zone J. 17, doi:10.2136/vzj2018.03.0052.

Lambot, S., Slob, E., van den Bosch, I., Stockbroeckx, B., Vanclooster, M., 2004. Modeling of ground-penetrating radar for accurate characterization of subsurface electric properties. IEEE Trans. Geosci. Remote Sens. 42, 2555?–2568.

Ledieu, J., Ridder, P.D., Clerck, P.D., Dautrebande, S., 1986. A method of measuring soil moisture by time-domain reflectometry. J. Hydrol. 88, 319–328.

Looyenga, H., 1965. Dielectric constants of heterogeneous mixtures. Physica 31, 401–406.

Malicki, M., Plagge, R., Roth, C., 1996. Improving the calibration of dielectric tdr soil moisture determination taking into account the solid soil. Eur. J. Soil Sci. 47, 357–366.

Olmi, R., Bittelli, M., 2015. Dielectric data analysis: recovering hidden relaxations by fourth-order derivative spectroscopy. IEEE Transactions on Dielectrics and Electrical Insulation 22, 3334–3340.

Pereira, M., Rial, F.I., Lorenzo, H., Arias, P., 2005. Analysis and calibration of gpr shielded antennas, IEEE, Delft, The Netherlands, p. DOI: 10.1109/AGPR.2005.1487878.

Rodriguez-Lado, L., Rial, M., Taboada, T., Cortizas, A.M., 2015. A pedotransfer function to map soil bulk density from limited data. Procedia Environmental Sciences 27, 45–48.

Roth, C.H., Malicki, M.A., Plagge, R., 1992. Empirical evaluation of the relationship between soil dielectric constant and volumetric water content as the basis for calibrating soil moisture measurements by tdr. J. Soil Sci. 43, 1–13.

Roth, K., Schulin, R., Fluhler, H., Attinger, W., 1990. Calibration of time domain reflectometry for water content measurement using a composite dielectric approach. Water Resour. Res. 26, 2267–2273.

Sandmeier, K.J., 2019. Reflex, GPR and seismic data processing software. Version 9.1. User Manual. https://www.sandmeier-geo.de/. Germany.

Schwing, M., Chen, Z., Scheuermann, A., Wagner, N., 2013. Dielectric properties of a clay soil determined in the frequency range from 1 mhz to 40 ghz, in: van Genuchten et al., M. (Ed.), Proc. of the 10th International Conference on electromagnetic Wave Interaction with Water and Moist Substances, ISEMA. Institute of Material Research and Testing at the Bauhaus University, Weimar, Germany, pp. 242–250.

Sihvola, A., 1999. Electromagnetic Mixing Formulas and Applications. Electromagn. waves ser. 47, ed., Inst. Electr. Eng., London.

Steelman, C.M., Endres, A.L., 2011. Comparison of petrophysical relationships for soil moisture estimation using gpr ground waves. Vadose Zone J. 10, 270?–285.

Steelman, C.M., Endres, A.L., Jones, J.P., 2012. High-resolution ground-penetrating radar monitoring of soil moisture dynamics: Field results, interpretation, and comparison with unsaturated flow model. Water Res. Resear. 48, doi:10.1029/2011WR011414.

Tillard, S., Dubois, J.C., 1995. Analysis of gpr data: Wave propagation velocity determination. J. Appl. Geophys. 33, 77–91.

Topp, G., Annan, J., Davis, A., 1980. Electromagnetic determination of soil water content: measurements in coaxial transmission lines. Water Res. Resear. 16, 574–582.

Weihermuller, L., Huisman, J.A., Lambot, S., Herbst, M., Vereecken., H., 2007. Mapping the spatial variation of soil water content at the field scale with different ground penetrating radar techniques. J. Hydrol. 340, 205–216.

***Declaration of Interest Statement**

Declaration of interests

☒ The authors declare that they have no known competing financial interests or personal relationships that could have appeared to influence the work reported in this paper.

☐The authors declare the following financial interests/personal relationships which may be considered as potential competing interests:

Figure Captions

1. Schematic of the plastic tank.
2. Picture of the soil within the plastic tank and GPR (Mala Inc., 800 MHz).
3. Example of radargram indicating the strong reflection from the metal plate.
4. Example of travel time determination on a representative trace.
5. Ground penetrating radar (GPR) permittivity with corresponding volumetric water contents collected for the sand, sandy loam, loamy sand and kaolinite clay textural classes. Points are gravimetric water contents and lines are estimated values for the four different models.
6. Scatter plot of measured and estimated data for the four soil types with linear relationships. Regression equations and coefficient of determinations are reported for the four equations.
7. Sensitivity analsyis for the parameter α.
8. Sensitivity analsyis for the parameter ϵ_s.

Figure1

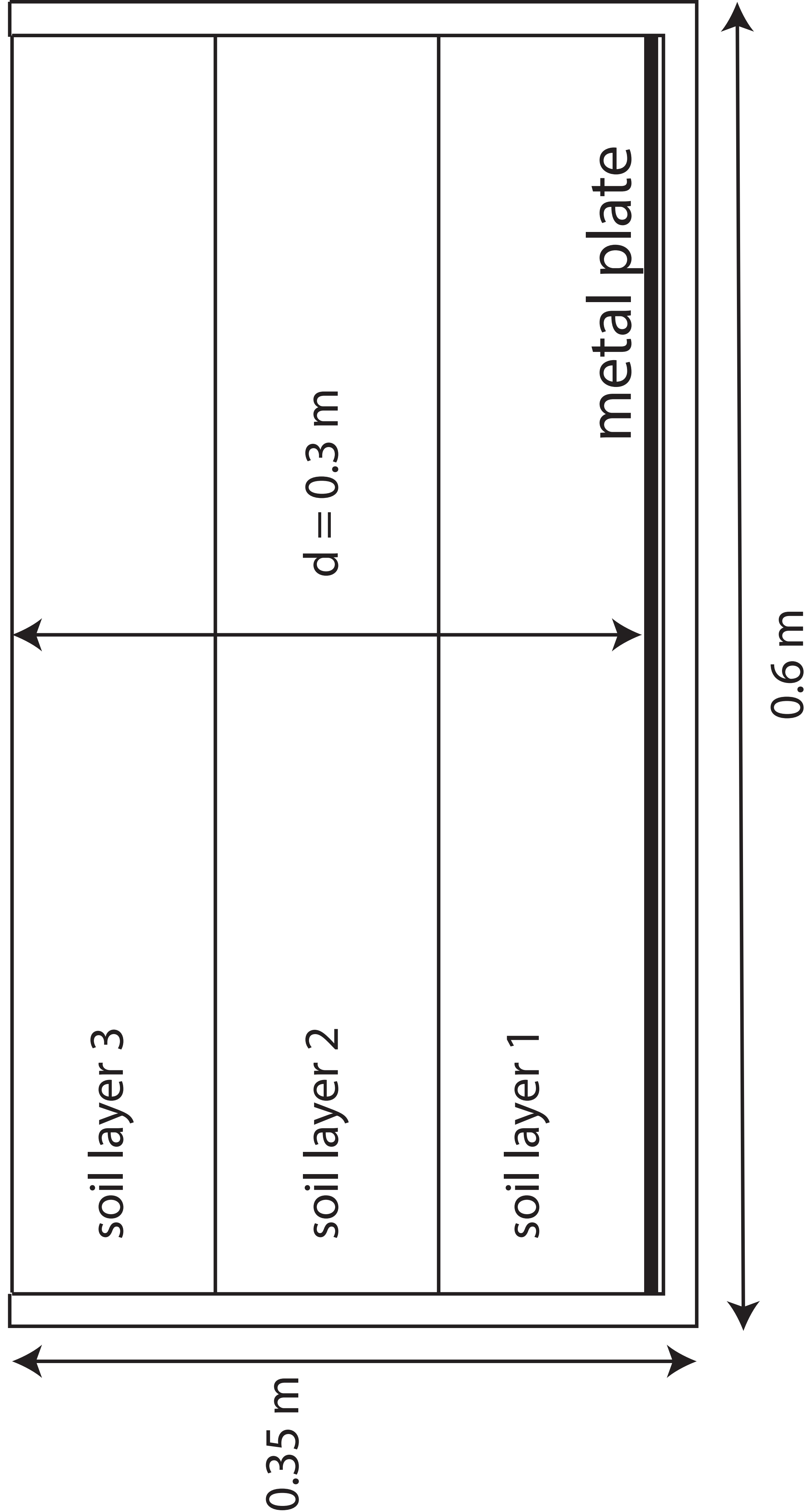

metal plate
d = 0.3 m
0.6 m
soil layer 3
soil layer 2
soil layer 1
0.35 m

Figure2

Figure3

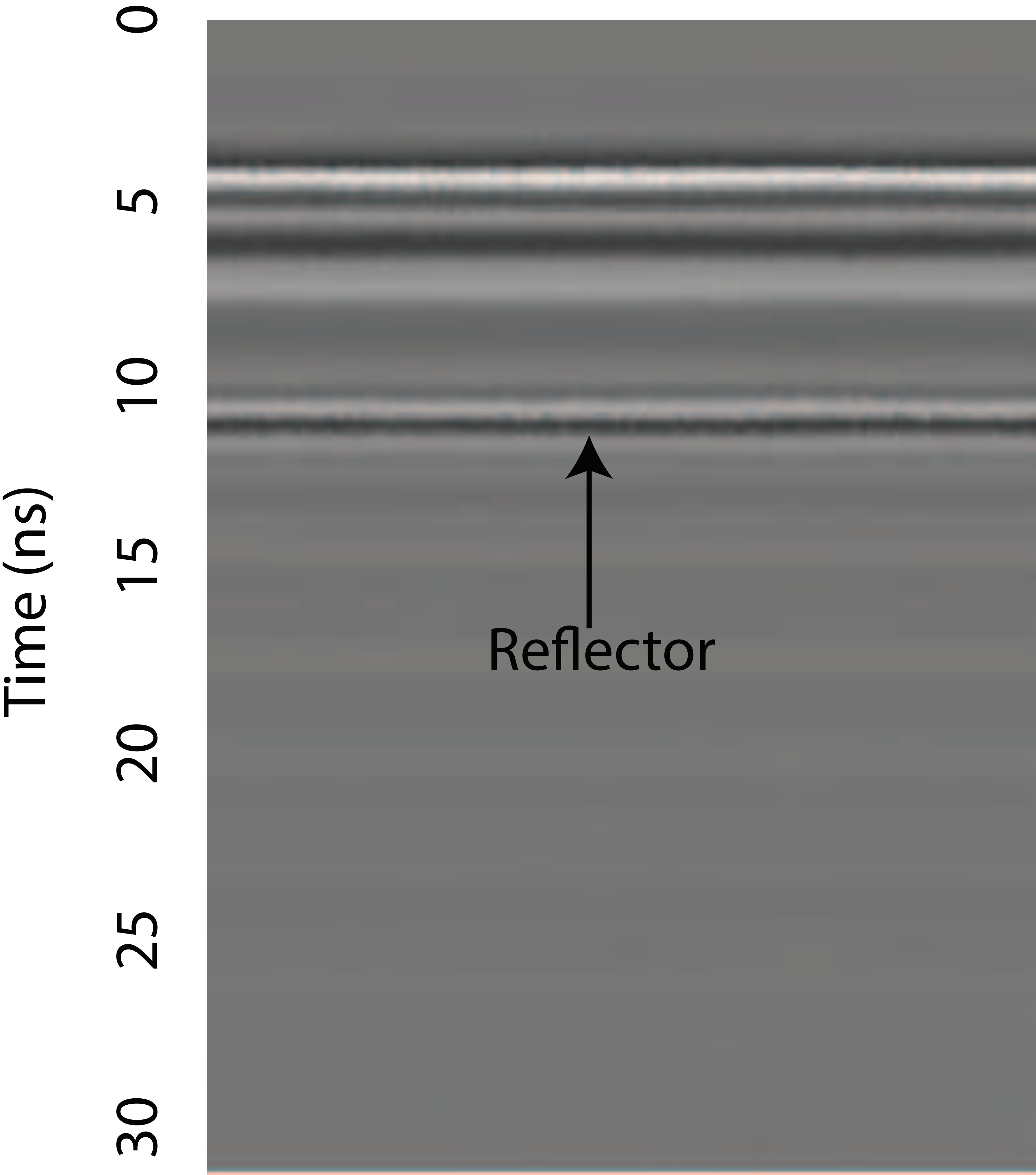

Figure 4

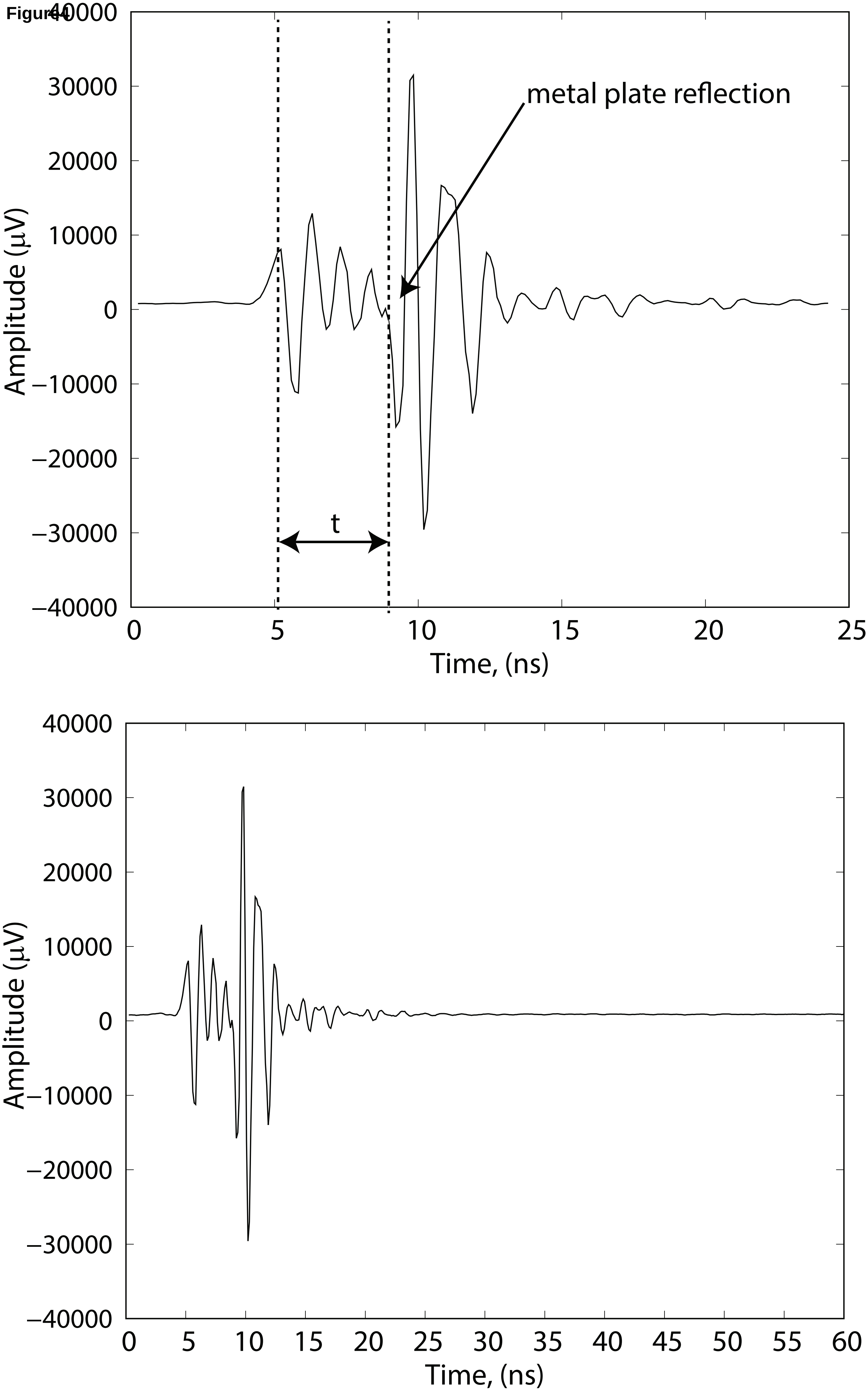
metal plate reflection
t
Amplitude (µV)
Time, (ns)
40000
30000
20000
10000
0
−10000
−20000
−30000
−40000
0
5
10
15
20
25
Amplitude (µV)
Time, (ns)
0
5
10
15
20
25
30
35
40
45
50
55
60

Figure5

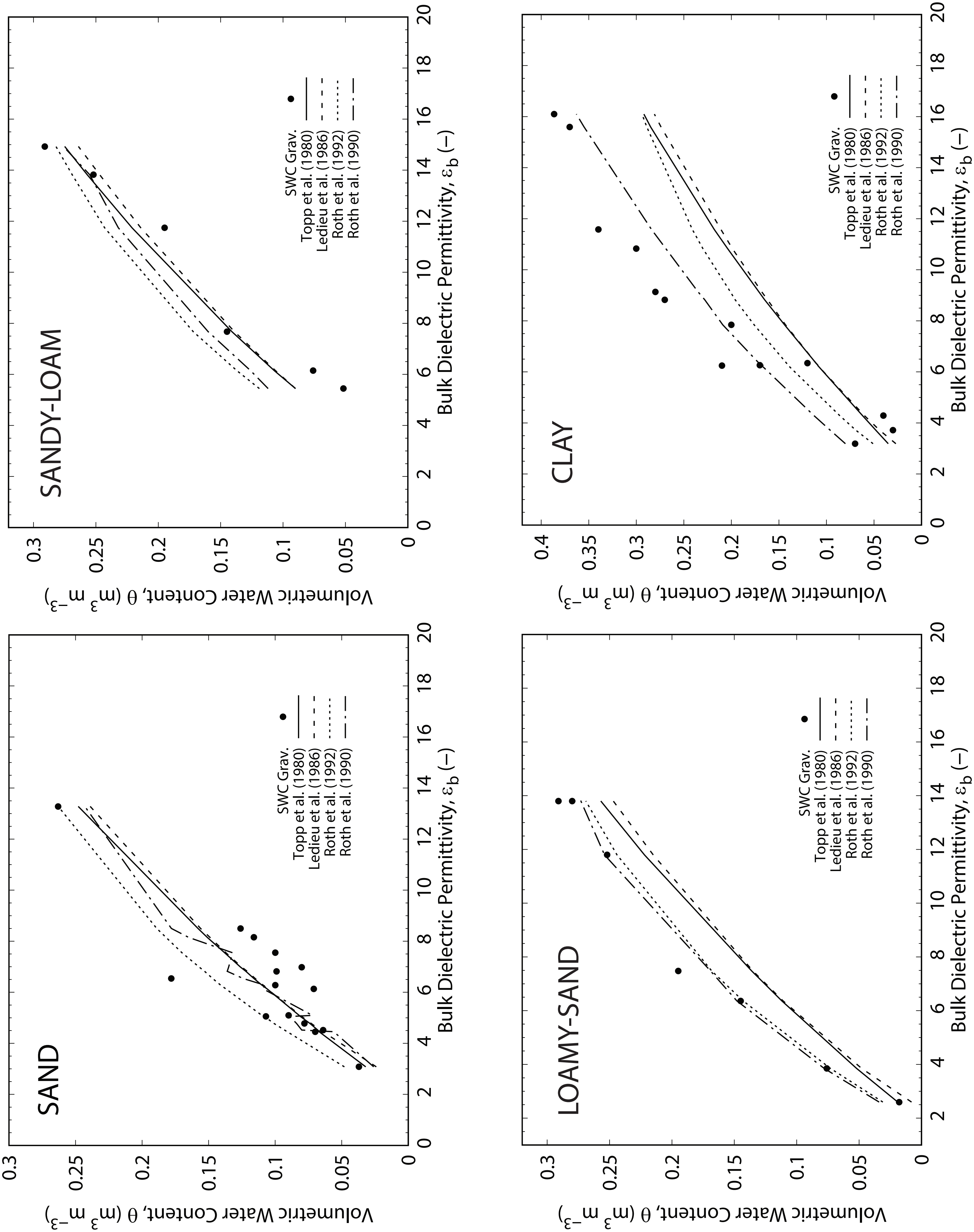
SAND
SANDY-LOAM
LOAMY-SAND
CLAY
SWC Grav.
Topp et al. (1980)
Ledieu et al. (1986)
Roth et al. (1992)
Roth et al. (1990)
Volumetric Water Content, θ (m³ m⁻³)
Bulk Dielectric Permittivity, εb (–)

Figure6

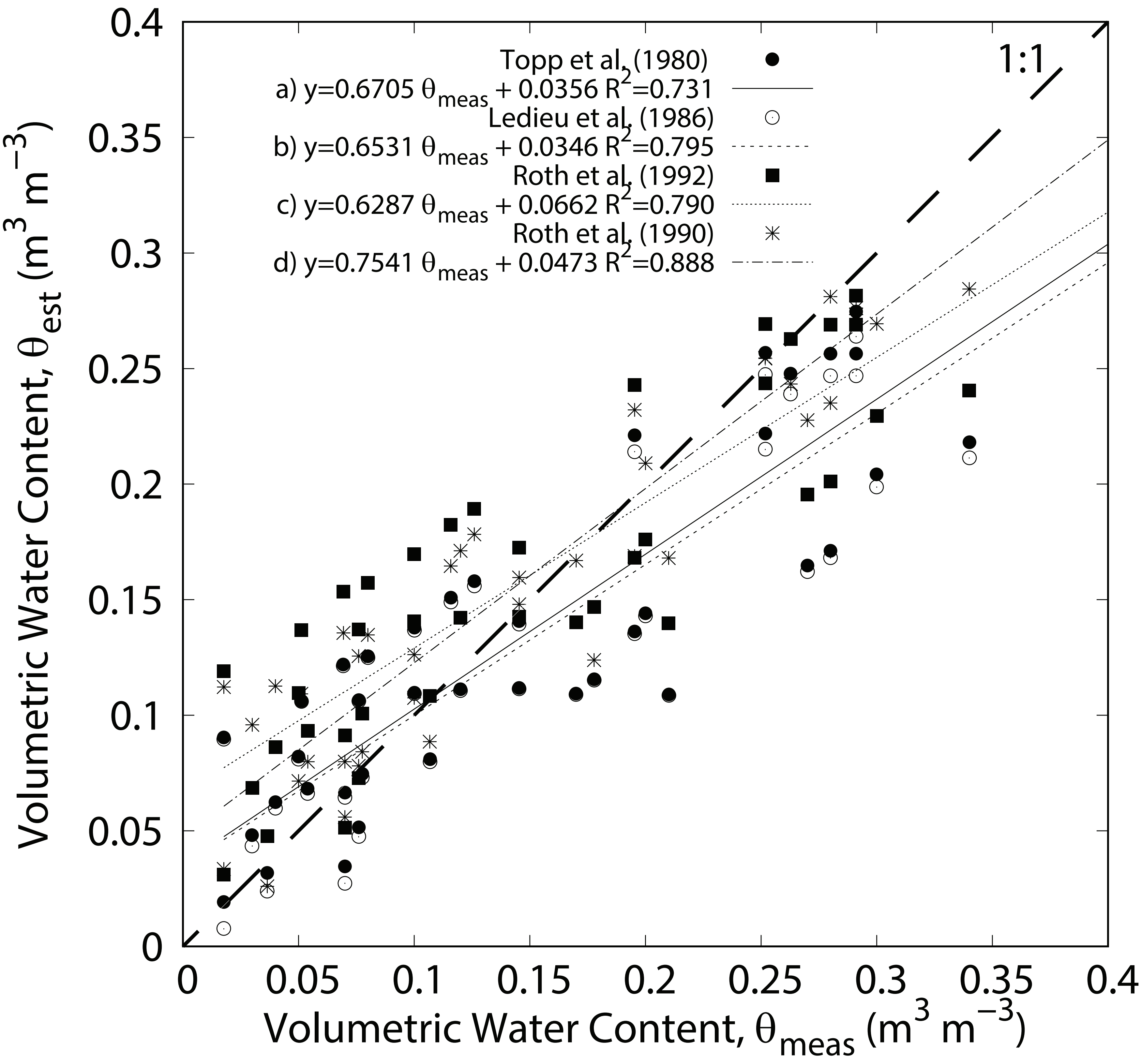

Topp et al. (1980)
a) y=0.6705 θmeas + 0.0356 R2=0.731
Ledieu et al. (1986)
b) y=0.6531 θmeas + 0.0346 R2=0.795
Roth et al. (1992)
c) y=0.6287 θmeas + 0.0662 R2=0.790
Roth et al. (1990)
d) y=0.7541 θmeas + 0.0473 R2=0.888
1:1
Volumetric Water Content, θest (m3 m−3)
Volumetric Water Content, θmeas (m3 m−3)
0
0.05
0.1
0.15
0.2
0.25
0.3
0.35
0.4

Figure7

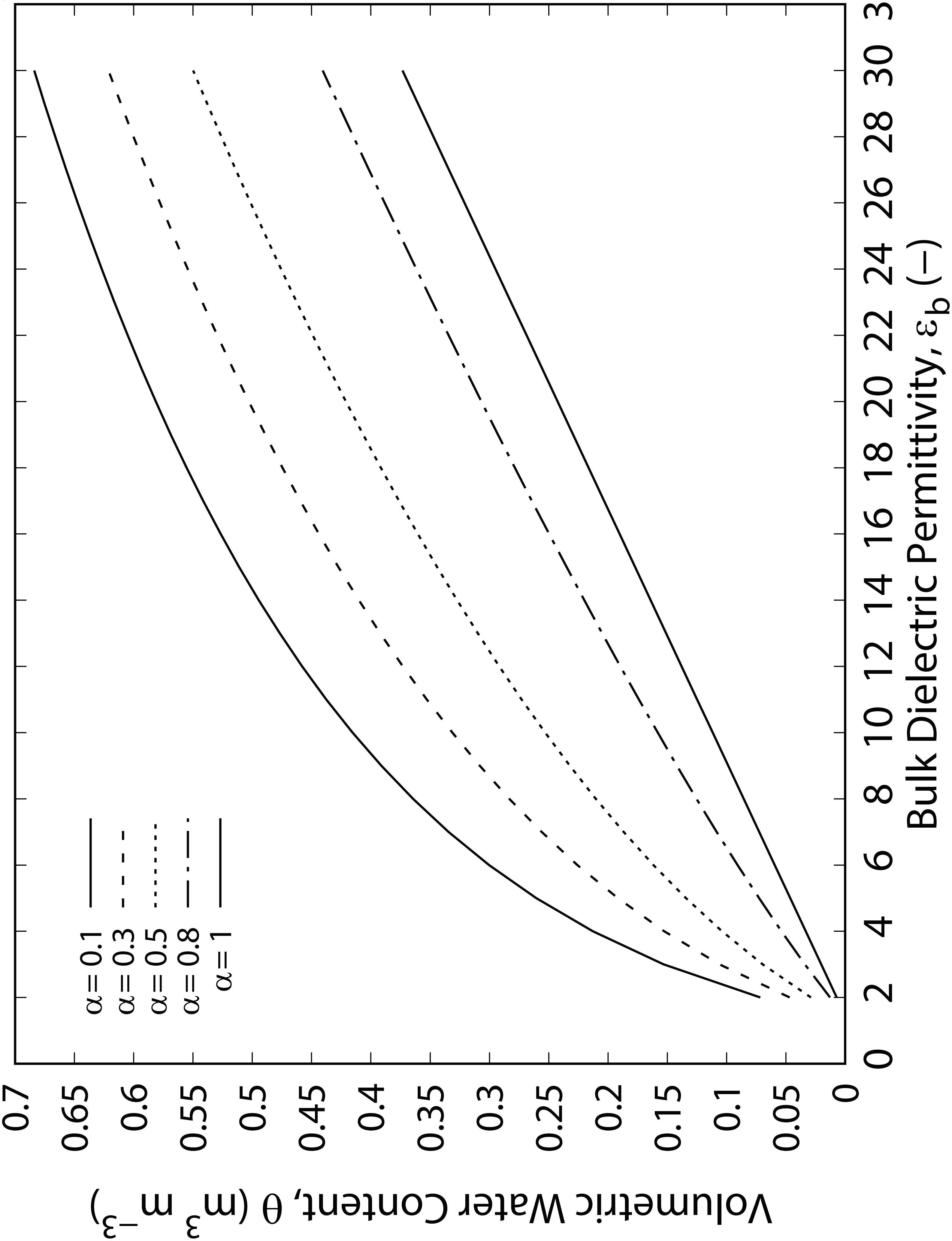
Volumetric Water Content, θ (m^3 m^−3)
Bulk Dielectric Permittivity, ε_b (–)
α = 0.1
α = 0.3
α = 0.5
α = 0.8
α = 1
0
0.05
0.1
0.15
0.2
0.25
0.3
0.35
0.4
0.45
0.5
0.55
0.6
0.65
0.7
2
4
6
8
10
12
14
16
18
20
22
24
26
28
30
32

Figure8

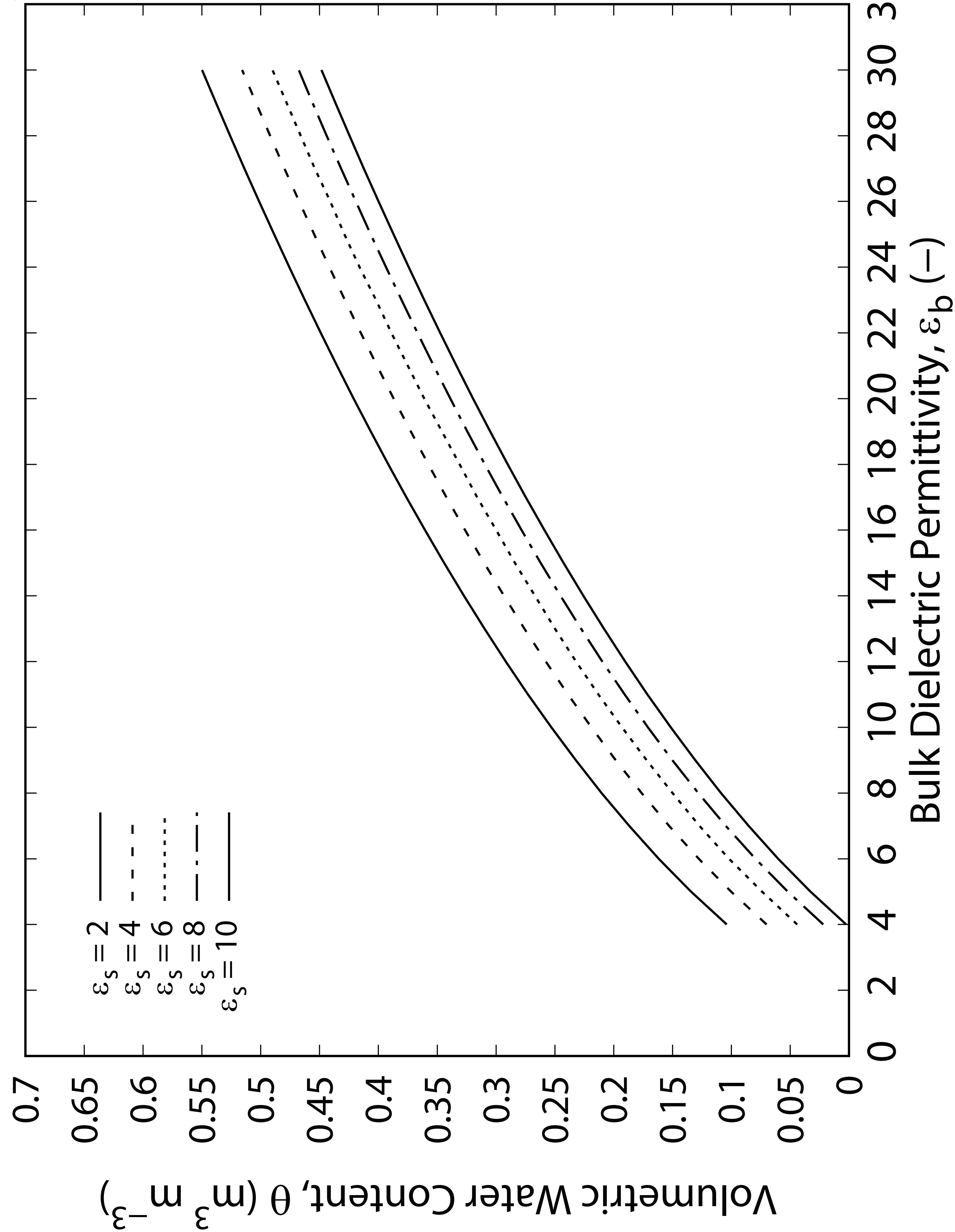

Volumetric Water Content, θ (m³ m⁻³)
Bulk Dielectric Permittivity, εb (–)
εs = 2
εs = 4
εs = 6
εs = 8
εs = 10
0 2 4 6 8 10 12 14 16 18 20 22 24 26 28 30 32
0 0.05 0.1 0.15 0.2 0.25 0.3 0.35 0.4 0.45 0.5 0.55 0.6 0.65 0.7